

# Search for clusters at high redshift

## I. Candidate Ly $\alpha$ emitters near 1138–262 at $z = 2.2$

J.D. Kurk<sup>1</sup>, H.J.A. Röttgering<sup>1</sup>, L. Pentericci<sup>2</sup>, G.K. Miley<sup>1</sup>, W. van Breugel<sup>3</sup>, C.L. Carilli<sup>4</sup>, H. Ford<sup>5</sup>, T. Heckman<sup>5</sup>, P. McCarthy<sup>6</sup>, and A. Moorwood<sup>7</sup>

<sup>1</sup> Sterrewacht Leiden, P.O. Box 9513, 2300 RA, Leiden, The Netherlands

<sup>2</sup> Max-Planck-Institut für Astronomie, Königstuhl 17, D-69117, Heidelberg, Germany

<sup>3</sup> Lawrence Livermore National Laboratory, P.O. Box 808, Livermore CA, 94550, USA

<sup>4</sup> NRAO, P.O. Box 0, Socorro NM, 87801, USA

<sup>5</sup> Dept. of Physics & Astronomy, The Johns Hopkins University, 3400 North Charles Street, Baltimore MD, 21218-2686, USA

<sup>6</sup> The Observatories of the Carnegie Institution of Washington, 813 Santa Barbara Street, Pasadena CA, 91101, USA

<sup>7</sup> European Southern Observatory, Karl-Schwarzschild-Str. 2, D-85748, Garching bei München, Germany

Received March 13, 2000; accepted May 2, 2000

**Abstract.** Radio, optical and X-ray observations of the powerful radio galaxy PKS 1138–262 at  $z = 2.156$  have suggested that this galaxy is a massive galaxy in the center of a forming cluster. We have imaged 1138–262 and the surrounding 38 square arcminute field with the Very Large Telescope<sup>a</sup> in a broad band and a narrow band encompassing the redshifted Ly $\alpha$  emission. We detect 50 objects with rest equivalent width larger than 20 Å and a luminous, highly extended Ly $\alpha$  halo around 1138–262. If the radio galaxy is at the center of a forming cluster, as observations at other wavelengths suggest, these objects are candidate Ly $\alpha$  emitting cluster galaxies.

**Key words:** Galaxies: active – Galaxies: clusters: general – Galaxies: evolution – Galaxies: luminosity function – Cosmology: observations – Cosmology: early Universe

### 1. Introduction

Observations of clusters at high redshift ( $z > 2$ ) can directly constrain cosmological models (e.g. Bahcall & Fan 1998), but searches based on colours or narrow band emission have not established the presence of massive clusters (Le Fèvre et al. 1996; Pascarelle et al. 1996; Keel et al. 1999). There are several indications (e.g. Pentericci et al. 1999) that powerful radio galaxies at high redshift (HzRGs) tend to be in the center of forming clusters. The powerful radio galaxy PKS 1138–262 at redshift 2.156 is a prime example of a forming brightest cluster galaxy and has extensively been studied (e.g. Pentericci et al. 1997). The arguments for 1138–262 being at the center

of a cluster include (a) the very clumpy morphology as observed by the HST (Pentericci et al. 1998), reminiscent of a massive merging system; (b) the extremely distorted radio morphology and the detection of the largest radio rotation measures ( $6200 \text{ rad m}^{-2}$ ) in a sample of more than 70 HzRGs, indicating that 1138–262 is surrounded by a hot, clumpy and dense magnetized medium (Carilli et al. 1997; Pentericci et al. 2000); (c) the detection of X-ray emission around 1138–262 (Carilli et al. 1998), indicating the presence of hot cluster gas, although a contribution to the X-ray luminosity by the AGN cannot be precluded. For this reason, we chose 1138–262 to carry out a pilot study with the VLT, to search for direct evidence of clusters at high redshift. There are various techniques for detecting high redshift companion galaxies. The colour selection technique used to find Lyman Break Galaxies (LBGs) (Steidel & Hamilton 1992) is not feasible at the redshift of 1138–262, since the Lyman limit falls at 2878 Å, which is well below the atmospheric cutoff. Therefore we have adopted the strategy of narrow band imaging at the wavelength of the redshifted Ly $\alpha$  line. This technique is capable of detecting galaxies at redshifts similar to the radio galaxy redshift having strong Ly $\alpha$  emission.

### 2. Observation, data reduction and calibration

Narrow and broad band imaging was carried out on April 12 and 13, 1999 with the 8.2m VLT Antu (UT1) using FORS in imaging mode. A narrow band filter was used which has a central wavelength of 3814 Å and a FWHM of 65 Å. For 1138–262 the emission of Ly $\alpha$  at 1216 Å is redshifted to 3838 Å, which falls within the range of the narrow band filter. The broad band filter was a Bessel B with central wavelength of 4290 Å and a FWHM of 880 Å, which receives both continuum and redshifted Ly $\alpha$  line emission. The detector was a Tektronix CCD with

*Send offprint requests to:* J.D. Kurk (kurk@strw.leidenuniv.nl)

<sup>a</sup> Based on observations carried out at the European Southern Observatory, Paranal, Chile, programme P63.O-0477(A).

2048<sup>2</sup> pixels and a scale of 0.2'' per pixel. Eight separate 30 minutes exposures were taken in narrow band and six 5 minutes exposures in B, shifted by  $\sim 20''$  with respect to each other to minimize flat fielding problems and to facilitate cosmic ray removal. The average seeing was 0.8'' and the 1 $\sigma$  limiting AB magnitude per square arcsecond was 27.8 for the narrow and 28.1 for the broad band image.

Image reduction was carried out using the IRAF reduction package. The individual images were bias subtracted and flat fielded by twilight flat fields for the narrow band and an average of the unregistered science exposures for the broad band. The images were then registered by shifting them in position by an amount determined from the location of several stars on the CCD. The registered images were co-added and cosmic rays removed. To improve the signal to noise and the sensitivity to faint extended objects, the resulting images were smoothed with a Gaussian function having a FWHM of 1''. The spectrophotometric standard star GD108 (Oke 1990) was used to calibrate the fluxes in broad and narrow band. Calibration in broad band is accurate to 0.1 magnitude, but absorption lines and a small break in the part of the spectrum of GD108 which falls in the narrow band inhibits equally accurate calibration for this filter. Instead, it was assumed that the spectrum is flat in this wavelength range and the narrow band is calibrated relative to the broad band with an accuracy of 0.2 magnitude, as estimated from the spectrum of GD108. We assume that the median equivalent width (EW) of a random sample of objects is equal to zero. Since the median EW of our sample calibrated by the standard star is equal to  $0.5 \times 10^{-19} \text{ erg s}^{-1} \text{ cm}^{-2} \text{ \AA}^{-1}$ , we subtract this number from the narrow band flux densities of the extracted objects to compute the EW. In this way, we do not rely on the absolute flux calibration.

### 3. Photometry and selection of Ly $\alpha$ emitters

Detection and photometry of objects in the field around 1138–262 was carried out using SExtractor (Bertin & Arnouts, 1996). We have taken advantage of all observing time by normalizing and adding the narrow and broad band images to obtain maximum signal to noise for the majority of objects, which resulted in the extraction of 1727 sources. All detections have at least 9 connected pixels with a value equal or larger than 2.5 times the rms sky noise. During this first application of SExtractor, aperture sizes and shapes were determined for each object separately. We gave the choice of aperture careful consideration by comparing the signal-to-noise for fixed circular apertures with a range of sizes and for elliptical apertures with a range of scale factors. The half lengths of the principal axes of the elliptical apertures are  $\epsilon kr_1$  and  $kr_1/\epsilon$ , where  $\epsilon$  is the ellipticity determined by the isophots of the object,  $r_1$  the first moment of the radial (non-elliptical) light distribution and  $k$  a scale factor. The highest average signal-to-noise for faint objects was obtained with

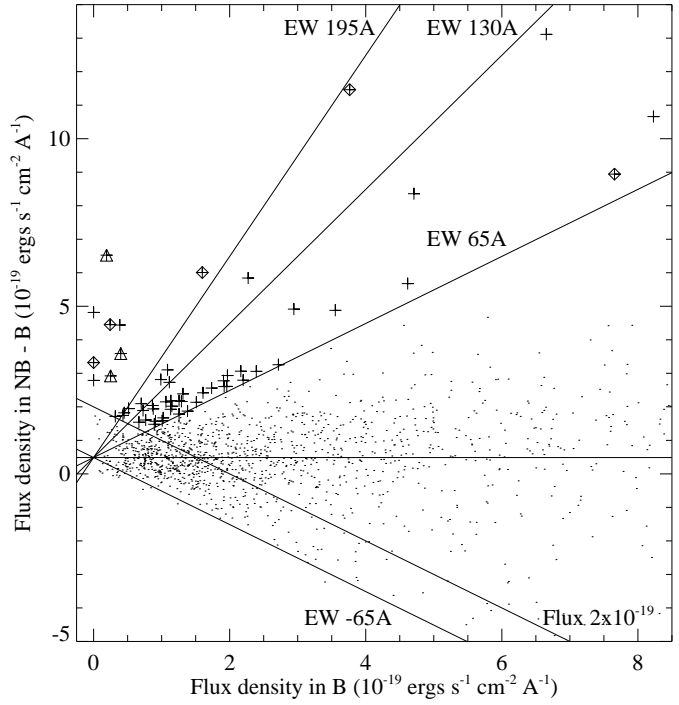


**Fig. 1.** Flux densities of extracted objects are shown as dots. Plus signs represent 55 objects selected as narrow band emitters, diamonds are part of the Ly $\alpha$  halo of 1138–262 (5 are not shown since they have flux densities up to  $8 \times 10^{-18} \text{ erg s}^{-1} \text{ cm}^{-2} \text{ \AA}^{-1}$ , exceeding the range of this plot) and triangles are the examples shown in Fig. 3. Straight lines of EW 195, 130 and 65  $\text{\AA}$  divide the region of candidates in strong (13), average(11) and weak emitters (36). Also shown are lines of EW -65  $\text{\AA}$ , narrow band flux density  $2 \times 10^{-19} \text{ erg s}^{-1} \text{ cm}^{-2} \text{ \AA}^{-1}$  and the median NB – B flux density of all extracted objects.

elliptical apertures using  $k = 1.25$ . The apertures determined in this way were used to carry out photometry on the narrow and broad band images.

Objects displaying twice as much flux density in the narrow band as in broad band have EW 65  $\text{\AA}$ . This equals to a rest frame EW of 20.5  $\text{\AA}$ , very close to the 20  $\text{\AA}$  used as selection criterium by Steidel et al. (1999, S99). There are 60 objects with EW larger than 65  $\text{\AA}$  and narrow band flux density of at least  $2 \times 10^{-19} \text{ erg s}^{-1} \text{ cm}^{-2} \text{ \AA}^{-1}$ . The signal-to-noise of these objects is at least 10 in narrow band, making the EW computation meaningful. We consider these to be candidate Ly $\alpha$  emitting galaxies. We subdivide the candidates in very promising ones with EW three times this value (13) and promising ones with EW two times this value (11), as shown in Fig. 1. Ten candidates coincide with peaks in the extended ( $\sim 160$  kpc<sup>b</sup>) halo of ionized hydrogen around the radio galaxy. So in total, there are 50 previously unknown emitters with a range of narrow band fluxes from 0.1 to  $5 \times 10^{-16} \text{ ergs s}^{-1} \text{ cm}^{-2}$ . The positions of the emitters are shown in Fig. 2. Images of three candidates are shown in Fig. 3.

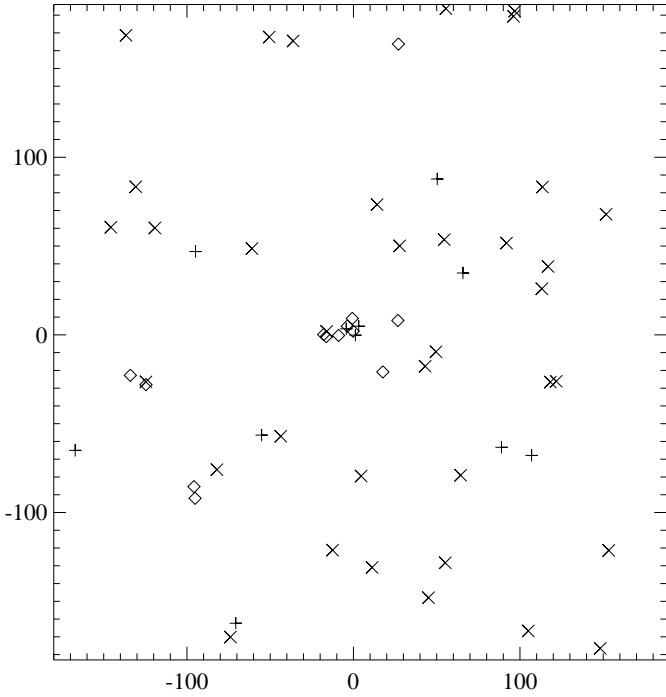


**Fig. 2.** Relative positions in arcseconds of the 60 narrow band emitters (including sources in the halo of 1138–262) in the final registered image. The center of the image is at RA 11<sup>h</sup>40<sup>m</sup>47.9, dec -26°29'08" (J2000). Diamonds, plus signs and crosses are emitters with EW respectively higher than 195, 130 and 65 Å. The Ly $\alpha$  halo of the radio galaxy is visible as a concentration of symbols in the center of the image.

We believe that there will be few or no low redshift interlopers, since [O II] $\lambda 3727$  at redshift 0.02 is the only strong line which falls in the narrow band filter, apart from Ly $\alpha$  at redshift 2.14. Galaxies at redshift 0.02 would easily be identified by their large angular size. Since the narrow band is positioned on the blue side of the broad band, our sample will not be contaminated by objects with abnormal colors as Extremely Red Objects or red M dwarfs or by objects with a break in their spectrum around 3900 Å as LBGs at  $z \sim 3.3$ . Contamination by bright quasars will be small, since their surface density ( $0.04 \text{ arcmin}^{-2}$ ; Thompson et al. 1999) is low enough that not more than 2 quasars will appear in our field. Although there still is a possibility that we have selected some rare, very blue objects with  $U - B < -1.3$ , we shall assume for the remainder of this paper that all objects with  $EW > 65 \text{ \AA}$  are Ly $\alpha$  emitting galaxies.

#### 4. Clustering analysis

Is there an enhanced density of galaxies around 1138–262?  
Do the candidates make up a forming cluster?

<sup>b</sup> Throughout this article, we adopt a Hubble constant of  $H_0 = 50 \text{ km s}^{-1} \text{Mpc}^{-1}$  and a deceleration parameter of  $q_0 = 0.5$ .

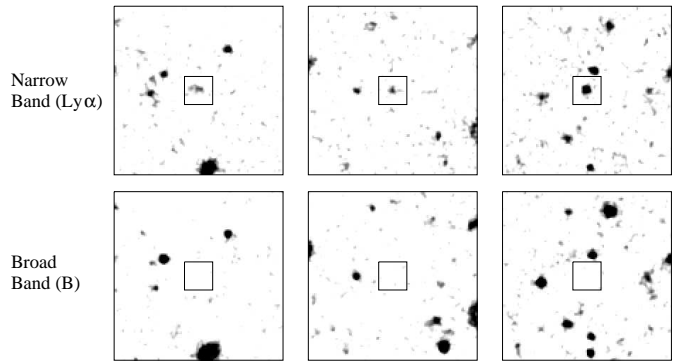


**Fig. 3.** Three probable cluster companions shown at the top in narrow band (Ly $\alpha$ ) and at the bottom in broad band (B).

The number of 50 Ly $\alpha$  emitters in the 35.4 arcmin $^2$  field ( $\sim 2.3 \text{ arcmin}^2$  is rendered unusable by bright stars) is equivalent to a surface density of 1.4 per arcmin $^2$ . The comoving volume for this field size ( $8.3 \text{ Mpc}^3$ ) and redshift range ( $2.110 \leq z \leq 2.164$ ) is  $4758 \text{ Mpc}^3$ , resulting in a volume density of  $1.1 \times 10^{-2}$  emitters per Mpc $^3$ . A contour plot of surface density does not show a strong concentration of emitters centered on the radio galaxy or anywhere else in the field.

The angular two point correlation function was determined by the Landy-Szalay estimator (Landy & Szalay 1993). Due to the occurrence of close pairs in our sample, the correlation function shows a signal at short distances, but there is no evidence that the distribution of emitters is significantly different from a random distribution on scales larger than 20''.

S99 present an overview of luminosity functions of three Ly $\alpha$  emission searches in their Fig. 5. We have converted our Ly $\alpha$  luminosities to star formation rate (SFR) using the relation  $L_\nu(1500\text{\AA}) = 8.0 \times 10^{27} (\text{SFR} / M_\odot \text{yr}^{-1}) \text{ ergs s}^{-1} \text{ Hz}^{-1}$  (Madau et al. 1998) and computed the number of emitters (omitting the radio galaxy halo objects) per SFR bin per Mpc $^3$  assuming  $z = 2.14$  for all emitters. The central wavelength of the B filter is 1366 Å in the restframe, which is close enough to 1500 Å to omit a K-correction carried out with an uncertain spectral index. Fig. 4 shows that the density of the cluster companions of 1138–262 (plus signs with vertical error bars) is comparable to the near-QSO search of Campos et al. (1999) at  $z = 2.6$ , which represents a small overdensity relative to the blank field search of Cowie & Hu (1998) at  $z = 3.4$ . The density is, however, lower than the Lyman break galaxy *spike* of S99 at  $z = 3.1$ . We have assumed that properties of forming clusters and galaxies do not change too fast to allow meaningful comparison between clusters at different epochs. The figure also shows that we detect SFR as low as  $1 \text{ h}^{-2} M_\odot \text{ yr}^{-1}$ , while Cowie & Hu (1998) and S99 reach their sensitivity limit at about  $8 \text{ h}^{-2} M_\odot \text{ yr}^{-1}$ . This is due, in part, to our sampling of a lower redshift range.

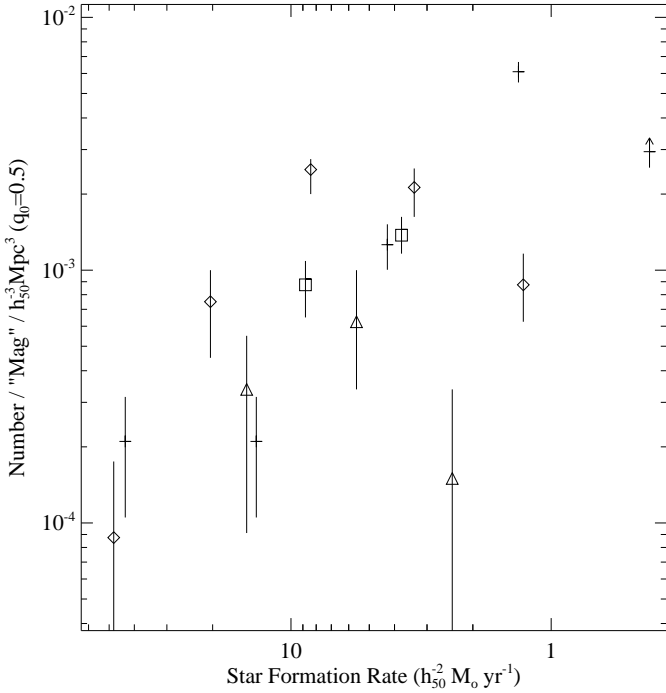


**Fig. 4.** The luminosity function of our Ly $\alpha$  emission selected objects at  $z = 2.2$  (+), Cowie & Hu's (1998) blank field narrow band emitters at  $z = 3.4$  ( $\triangle$ ), Campos et al.'s (1999) near-QSO search at  $z = 2.6$  ( $\square$ ) and S99's overdensity of star forming galaxies at  $z = 3.1$  ( $\diamond$ ). Note that our bin with the lowest SFR is only a lower limit, due to sensitivity incompleteness. Figure reproduced from S99.

## 5. Discussion

Although we have detected a number of Ly $\alpha$  emitters in the field of 1138–262, from the present data it is impossible to unambiguously determine whether a significant fraction of these objects form part of the presumed cluster around 1138–262. Note that the observations described here can only detect galaxies with bright Ly $\alpha$  emission lines not attenuated by dust and these might comprise merely a small fraction of the galaxy content of the presumed cluster. First, of the whole population of LBGs as studied by S99 only 20% have a Ly $\alpha$  rest EW 20 Å. About 50% of the LBGs have the Ly $\alpha$  region even in absorption. Second, only a fraction of the cluster galaxies are likely to be actively forming stars. We assume that the ratio of early to late type galaxies in the cluster around 1138–262 is the same as the 1.1:1 ratio in intermediate redshift ( $z \sim 0.5$ ) clusters as found by Andreon (1998). Taking these two factors into account, the detected Ly $\alpha$  galaxies might comprise only 10% of the cluster galaxies present around 1138–262. In addition to this, we miss galaxies emitting Ly $\alpha$  outside the limited range of wavelength covered by our narrow band filter. Assuming that the radio galaxy is at rest with respect to the cluster, the wavelength of Ly $\alpha$  from galaxies with a positive velocity greater than 860 km s $^{-1}$  falls

outside the FWHM of the filter. Since present day clusters have velocity dispersions as large as  $\sim 1200$  km s $^{-1}$  (Mazure et al. 1996), we miss 15% of the velocity range of the presumed cluster around 1138–262 if we assume the same velocity dispersion for clusters at high redshift.

## 6. Conclusions

We have detected 50 candidate Ly $\alpha$  emitters close to radio galaxy 1138–262 at redshift 2.2. These Ly $\alpha$  emitters are candidate starburst galaxies in the cluster, which is presumed to exist or to be forming around 1138–262. We do not find a significant overdensity of candidates compared to luminosity functions of blank fields nor do we detect a strong concentration gradient in our 8 Mpc $^2$  field. The next step in our search for clusters at high redshift is to confirm the existence of the Ly $\alpha$  emitters by multi object spectroscopy at the VLT and determine the spatial correlation function and velocity dispersion, which together with the size of the cluster will give a direct estimate of the total mass. Additionally, we will carry out X-ray observations of 1138–262 with the Chandra telescope.

*Acknowledgements.* JK acknowledges productive discussions with Philip Best and Tom Thomas. The work by WvB at IGPP/LLNL was performed under the auspices of the US Department of Energy under contract W-7405-ENG-48. IRAF is distributed by the National Optical Astronomy Observatories, which are operated by the Association of Universities for Research in Astronomy, Inc., under cooperative agreement with the National Science Foundation.

## References

- Andreton S., 1998, ApJ 501, 533
- Bahcall N.A., Fan X., 1998, ApJ 504, 1
- Bertin E., Arnouts S., 1996, A&AS 117, 393
- Campos A., Yahil A., Windhorst R.A. et al., 1999, ApJ 511, L1
- Carilli C.L., Röttgering H.J.A., van Ojik R., Miley G.K., van Breugel W.J.M., 1997, ApJS 109, 1
- Carilli C.L., Harris D.E., Pentericci L. et al., 1998, ApJ 496, L57
- Cowie L.L., Hu E.M., 1998, AJ 115, 1319
- Le Fèvre O., Deltorn J.M., Crampton D., Dickinson M., 1996, ApJ 471, L11
- Keel W.C., Cohen S.H., Windhorst R.A., Waddington I., 1999, AJ 118, 2547
- Landy S.D., Szalay A.S., 1993, ApJ 412, 64
- Madau P., Pozzetti L., Dickinson M., 1998, ApJ 498, 106
- Mazure A., Katgert P., den Hartog R. et al., 1996, A&A 310, 31
- Oke J.B., 1990, AJ 99, 1621
- Pascarelle S.M., Windhorst R.A., Keel W.C., Odewahn S.C., 1996, Nature 383, 45
- Pentericci L., Röttgering H.J.A., Miley G.K., Carilli C.L., McCarthy P., 1997, A&A 326, 580
- Pentericci L., Röttgering H.J.A., Miley G.K. et al., 1998, ApJ 504, 139
- Pentericci L., Röttgering H.J.A., Miley G.K. et al., 1999, A&A 341, 329

Pentericci L., van Reeven W., Carilli C.L., Röttgering H.J.A.,  
2000, A&A in preparation

Steidel C.C., Hamilton D., 1992, AJ 104, 941

Steidel C.C., Adelberger K.L., Shapley A.E. et al., 1999, ApJ  
submitted, astro-ph/9910144 (S99)

Thompson D., Beckwith S.V.W., Fockenbrock R. et al., 1999,  
ApJ 523, 100